Journal of Materials Chemistry A

Accepted Manuscript

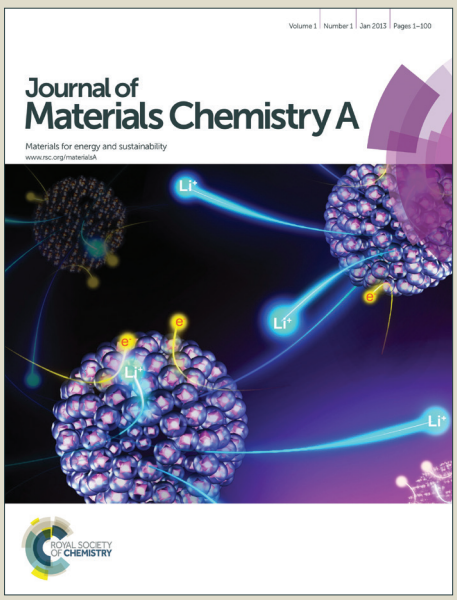

ROYAL SOCIETY OF CHEMISTRY

www.rsc.org/materialsA

Cite this: DOI: 10.1039/c0xx00000x

www.rsc.org/xxxxxx

ARTICLE TYPE

Controllable Synthesis of Uniform ZnO Nanorods and their Enhanced Dielectric and Absorption Properties **

Guang-Sheng Wang[a]*, Ying-Ying Wu[a], Xiao-Juan Zhang[a], Yong Li[b], Lin Guo[a]*, and Mao-Sheng Cao[b]*

Received (in XXX, XXX) Xth XXXXXXXXX 20XX, Accepted Xth XXXXXXXXX 20XX
DOI: 10.1039/b000000x

The enhanced dielectric properties of the ZnO/PVDF **nanocomposites resulted by the synthesized uniform ZnO nanorods (NR) were studied; the results indicate that the dielectric constant of the composites are obviously improved (196, at 10^2 Hz) with lower percolation threshold (Volume 0.0548); percolation theory is employed to explain the enhanced dielectric properties; the stability of the dielectric constants of percolation composites with the temperature from 20 °C to 140 °C was also studied. While, the enhanced wave absorption properties of the composites were also investigated, and with the filler content 10 wt%, the reflection loss appears two peaks that can reach -15.90 dB at 6.60 GHz and -25.44 dB at 16.48 GHz, respectively. The increased mechanism of absorption properties was also explained in detail.**

1. Introduction

As an important wide-band-gap semiconductor with Eg=3.37 *eV*, ZnO has always been the hot topic as a result of its unique applications in catalysts, sensors, piezoelectric transducers and actuators, and photovoltaic and surface acoustic wave devices.[1, 2] And for these reasons, as a most important morphology, the controlling of one-dimensional ZnO structure is critical to practical application; various synthetic methods have been developed to prepare one-dimensional ZnO nanomaterials, such as vapor–liquid–solid epitaxial (VLSE) mechanism,[3] thermal evaporation,[4] hydrothermal methods,[5] template-based growth,[6] chemical vapor deposition,[7] pulsed laser deposition[8] and micro-emulsion,[9] etc. among these methods, the hydrothermal methods is the most probable to synthesize one-dimensional ZnO nanomaterials in large quantity and can satisfy the industrial production, however, the investigation of the reaction parameters of hydrothermal method and optimum reaction conditions is still a challenge to control synthesis of one-dimensional ZnO nanomaterials in large quantity at low temperature.

In the last decade, the percolative composites have been developed and the conductive filler/polymer composite is an approach towards high dielectric constant materials based on percolation theory. Various conductive fillers, such as silver (Ag),[10] aluminum (Al),[11] zinc (Zn),[12] nickel (Ni), carbon black,[13] graphene based composites,[14] have been used to prepare the polymer-conductive filler composites or three-phase percolative composite systems.

Recently, ZnO nanoparticles have also attracted considerable attention in polymer community as fillers for the composites.[15-17] Nanoscale fillers are different from bulk materials and conventional micron-size fillers due to their small size and corresponding increase in surface area.[17-21] It is expected that the addition of ZnO nanoparticles into polymers would lead to unprecedented ability to control the electric properties of filled polymers. As commonly known, the ZnO/polymer composites were always thought as a material with low dielectric constants, and no percolation threshold was found by adding ZnO nanoparticles (49 nm) into low-density polyethylene (LDPE) even at high filler content.[22] The dielectric properties of composite depend on the preparation method, and interface interaction between the fillers and the polymer, especially the morphologies of fillers.[23, 24] New insights into the unique properties of the nanoparticles filler and polymer-matrix have been gained in most recent studies. For example, by dispersing semiconductor ZnO, in the form of radial nanowire clusters structure into the PVDF, a high dielectric constant in the neighborhood of the percolation threshold was obtained.[25] The percolation threshold concentration of the ZnO is low as 5.48 (Vol.), and the calculated percolation threshold is 0.661. However, for the percolation composite, with the addition of

conductive filler, the dielectric constants decrease rapidly with the increasing frequency and the dielectric loss increases rapidly too, the dielectric loss is higher than 0.5 in the low frequency. From the point of view of dielectric property, dielectric constant and dielectric loss are the two most important parameters that indicate the performance of a candidate material for embedded capacitors. How to increase the dielectric constant and decrease the dielectric loss is still a challenge.

On other hand, as a kind of wave absorber, semiconductor nanomaterials were also employed to settle with the increased pollution of electromagnetic waves.[26] A number of nanomaterials absorbing microwaves with specific morphology have been reported including carbon nanotubes SiC,[27] Fe, [28]Fe_3O_4, or TiO_2 encapsulated within carbon nanocomposites,[29] CdS/Fe_2O_3 with heterostructures，[30]MnO_2, [31] CuS, [32]etc. And the ZnO nanomaterials are widely studied for its excellent absorption properties, Cao and his coauthor[33-35] studied the absorption properties of ZnO whiskers, and got a series of excellent results. While, the absorption properties are mostly studied based on the composites of wax and nanomaterials at present stage, which limits the practical application of the composites. At the mean time, our recent studies indicated that inorganic-organic nanocomposites showed very strong wave-absorption abilities with promising application.[36] In our former work, PVDF is chosen as composite polymeric matrix materials in the fabrication of inorganic-organic nanocomposites because of its specific physical properties and excellent dielectric properties.[25, 31, 37, 38] Besides, our research also revealed the existence of synergic effect between PVDF and nanofillers,[36, 39] which could distinctly enhance the wave-absorption of nanocomposite.

Many factors will affect the properties of nanomaterials, such as morphology, synthesis method, etc. In this paper, we prepared ZnO nanorods (NR-ZnO) by a simple solvothermal method and investigated the dielectric and absorption properties of NR-ZnO/PVDF composites. The results showed that the addition of NR-ZnO, with a quite low percolation threshold, significantly improves the dielectric constant (196, at 10^2 Hz) of polymer matrix composites; at the same time, NR-ZnO powders were added as an absorber into PVDF to get excellent absorption properties with lower filler content, the enhanced mechanism was also studied.

2. Experimental Section

Commercially available and analytical-grade reagents were used without further purification. For a typical synthesis process: $Zn(CH_3COO)_2{\cdot}2H_2O$ (0.55 g) and cetrimonium bromide powder (0.1 g) were dissolved in the ethylene glycol (EG) 60 ml at room temperature. After the solution was vigorously stirred for 1 h at room temperature, 80% hydrazine hydrate with different amount of 6 ml, 8 ml, 12 ml, 20 ml, 25 ml, 30 ml were added respectively, and stirred for 1 h, then the solution was added to the autoclave and maintained at 160 °C for 6 h and cooled to room temperature naturally. The precipitation was washed with ethanol for several times, and then dried at 70 °C.

A series of PVDF were dissolved in 500 ml N-dimethylformamide (DMF) at room temperature. After the solution was transparent, the NR-ZnO were added, respectively, then dispersed them in fosters after the ultrasonic bath at room temperature. Then, dry them in the oven at 100 °C. The dried mixture was collapsed and compressed into wafers for 15 min at 200 °C under 10 MPa (pre-pressed for 5 min at the same temperature, released the press for a while, and then, re-pressed for 20 min, followed by cooling to room temperature under the same pressure).

Powder XRD data were collected on a Rigaku D/MAX 2200 PC automatic X-ray diffractometer with Cu Ka radiation (λ = 0.154056 nm). The grain morphology and size was observed by SEM (HITACHIS-4800). The dielectric constants are measured by a HP 4294A Impedance meter in the frequency range of 100/110 MHz, at an average voltage of 0.5 V from 20 °C to 140 °C temperature.

3.Results and Discussion

A general SEM overview of the as-prepared product (shown in **Figure 1**a) indicates that the product is mainly consisted of uniform ZnO nanorods. A magnified examination of the ZnO nanorods is shown in **Figure 1b**. All the products are uniform nanorods with the diameter about 60 nm and the length 250 nm. Additional structural characterization of the ZnO nanorods is carried out using TEM, HRTEM. The TEM image (shown in **Figure 1c and d)** shows the typical image of the ZnO nanorods, which are uniform and stable even after a long time treatment by ultrasonic. The inserted of Figure **1d**, which is selected area (marked by a red square) electron diffraction (SAED) pattern, indicates that the single nanorod is single crystal. HRTEM image (shown in **Figure 1e**), taken from a nanorod, shown in **Figure 1d** marked by a blue square reveals that the nanorods possess a single crystal hexagonal structure, and the lattice spacing of 0.162 nm corresponds to the lattice of (120) crystal planes. Powder XRD pattern of the typical products synthesized by Zn $(CH_3COO)_2{\cdot}2H_2O$ (0.55 g), 100 mg CTAB and 20 ml 80% hydrazine hydrate dissolved in the EG 60 ml and reaction at 160 °C for 6 hours is shown in **Figure 1f**. All of the diffraction peaks can be indexed as those from the known

Wurtzite-structured (hexagonal) ZnO (JCPDS No. 75-0576). No peaks for other phases were observed, thus indicating high purity and crystallinity of the products.

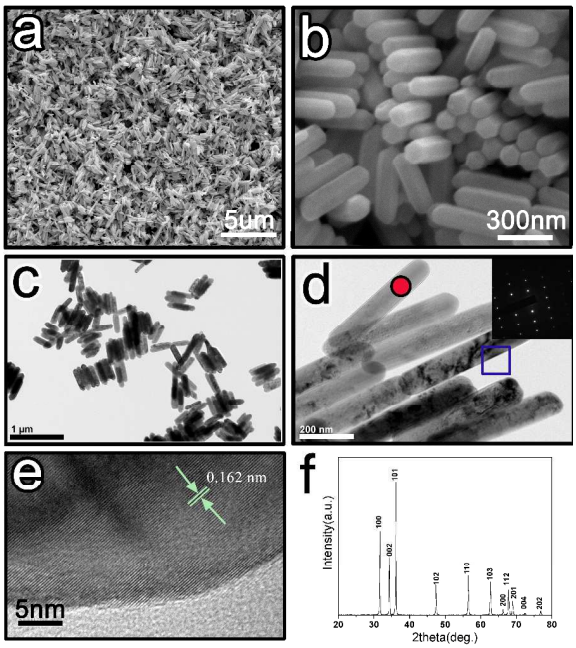

Figure 1. a) The SEM image overview of the as-prepared nanorods; b) the magnified SEM images of the products; c) the TEM image overview of the nanorods; d) the magnified TEM images of the products; e) the HRTEM image of the nanorod; f) XRD pattern of NR-ZnO; the inserted of d) is the SAED pattern.

The optimized reaction conditions to prepare NR-ZnO were also studied. From the previous report by our group,[40] in present reaction system, the amount of hydrazine hydrate plays a key role on the growth of ZnO nanorods. When the reaction is performed at the same condition only decreasing the hydrazine hydrate to 6 ml(shown in **Figure S1**a), the main structures of the products are spheres with the diameter about from 2 μm to 4 μm; when the amount of the hydrazine hydrate is 8 ml (shown in **Figure S1**b), the main structures are still spheres, but the spheres are connected by a certain number, looks as a big sphere split into the complicated structures; a more complicated nanostructures formed when the amount of the hydrazine hydrate is 12 ml (shown in **Figure S1**c), the structures are more like the nanorods bundles connected with a certain number; when the amount of the hydrazine hydrate is 20 ml (shown in **Figure S1**d), the products are uniform nanorods with the diameter about 60 nm and the length 250 nm; when the amount of hydrazine hydrate increased to 25 ml (shown in **Figure S1e**), the products are nanorods with the diameter 50-70 nm and length about 700-800 nm; when the amount of hydrazine hydrate increased to 30 ml (shown in **Figure S1f**), the products are still uniform nanorods with the diameter 50-70 nm and length about 1-1.5 μm. These results also indicate that the amount of hydrazine hydrate plays a key role to synthesize the uniform nanorods, which is a promising way to fabricate the uniform ZnO nanorods with different ratio of length/diameter in large scale.

To investigate the interior structure of the composites affected by the concentration of NR-ZnO, various contents of NR-ZnO were mixed with PVDF in DMF to form ZnO+PVDF solution and fabricate the films. The SEM images of composites in **Figure 2a, b, c and d** show that the composites are sandwich structure. There are two kinds of parallel layers in the composites; one is a pure inorganic layer and the other is a uniform composite layer, which is shown the magnified images in the corresponding pictures **Figure S2**. The inorganic layers were mainly congregated ZnO, which was due to the deposition of NR-ZnO in the dispersion process and there was no obvious change with the increasing content of NR-ZnO; the composites layer consisted of PVDF and dispersed NR-ZnO was shown in the inserted of the magnified images of square labeled in the corresponding pictures, in which the concentration of NR-ZnO increased with the content of filler. The NR-ZnO is still kept primary shape in the composites after the hot-press and the space among the NR-ZnO decreases with the increasing of the volume ratio of NR-ZnO/PVDF **(Figure S2b, d, and f)**. As the volume content reached 0.0776, some nanorods linked and formed local conducting materials (**Figure S2h**). To confirm the good dispersion of NR-ZnO in the composites, the results of XRD of the composites with different filler contents are shown in **Figure 2e**, in which the NR-ZnO and PVDF peaks diffractions are still observed in the nanocomposite. The FESEM characterization and elemental maps of PVDF/ZnO are also displayed in **Figure 2f**. The elemental maps of Zn, O, F and C, which are on the surface of the PVDF/ZnO nanocomposites also confirm the good dispersion of the NR-ZnO in PVDF. The selected magnified connected part of the NR-ZnO and PVDF is also given in the **Figure S3**, which further confirmed the good adhesion between inorganic NR-ZnO and the organic matrix, which is due to the usage of CTAB in the synthesis process. The good dispersion of the NR-ZnO in PVDF may be helpful for the dielectric and absorption properties. In addition, from the photograph of the ZnO/PVDF film in **Figure S4**, this film also exhibits excellent flexibility.

In order to compare the dielectric properties with the reference 18, the dielectric properties of various volume contents (volume contents 0.0163, 0.0345, 0.0548 and 0.0776

corresponding with the 5 wt%, 10 wt%, 15 wt% and 20 wt%) of NR-ZnO/PVDF composites were measured at room temperature, which is shown in **Figure 3a**.

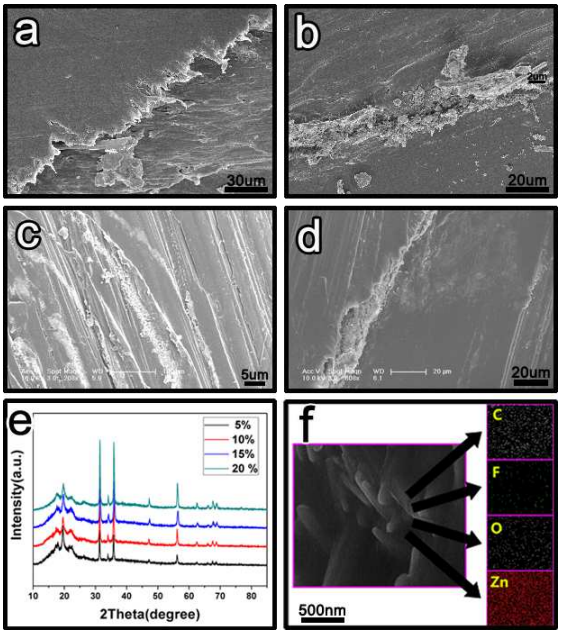

Figure 2. A cross-sectional SEM image of the wafers of the composite with the different volume ratio: a) 0.0163; b) 0.0345; c) 0.0548; d) 0.0776; the top inserted of the magnified were the ZnO layer images of square labeled in the corresponding images; the bottom inserted of the magnified were the composites layers images of square labeled in the corresponding images; e) XRD the composites with different filler contents; f) The elemental maps of Zn, O, F and C of the composites.

The dielectric constants of NR-ZnO/PVDF decrease with the increasing frequency; the high dielectric constant is visible at a critical volume concentration f_{NR-ZnO} =0.0548. The dielectric constants of NR-ZnO/PVDF increase with the filler content before abruptly increasing at a critical volume concentration f_{NR-ZnO} =0.0548 and then decrease. For example, the dielectric constants for the samples at the frequencies 10^3 Hz, 10^4 Hz and 10^5 Hz at room temperature are also shown in **Figure 3b**, respectively. The dielectric constant of the composite with f_{NR-ZnO} =0.0548 reaches 196 at 10^2 Hz, which is significantly higher than that of other reported composites with the radial ZnO nanowire clusters at the same filler content.[25] The dielectric constant of the composites with the addition of bulk-ZnO increases with the volume filler content and there exists no percolation threshold by adding ZnO nanoparticles into PVDF, which is reported in ZnO/LDPE[22] and R-ZnO/PVDF composite. Comparing with the dielectric constants of the bulk-ZnO/PVDF (the image of bulk-ZnO is shown in **Figure S5**) and R-ZnO/PVDF, it is obvious that the addition of NR-ZnO can also greatly improve the dielectric constant of pure PVDF (10, 10^2 Hz), for comparison, the result of the bulk-ZnO/PVDF with the volume content 0.0776 is also given in the **Figure 3a** and **Figure 3b**. This implies that the incorporation of ZnO nanorods into PVDF is very effective to increase its dielectric constant. For the composite, the dielectric loss increases rapidly compared to pure PVDF shown in **Figure 3c**. Usually, the introduction of inorganic fillers to a polymer matrix enhances the dielectric loss values of the composites, as there is an enhancement in the sources of charge carriers in the system induced by the electrically conductive NR-ZnO.[40]

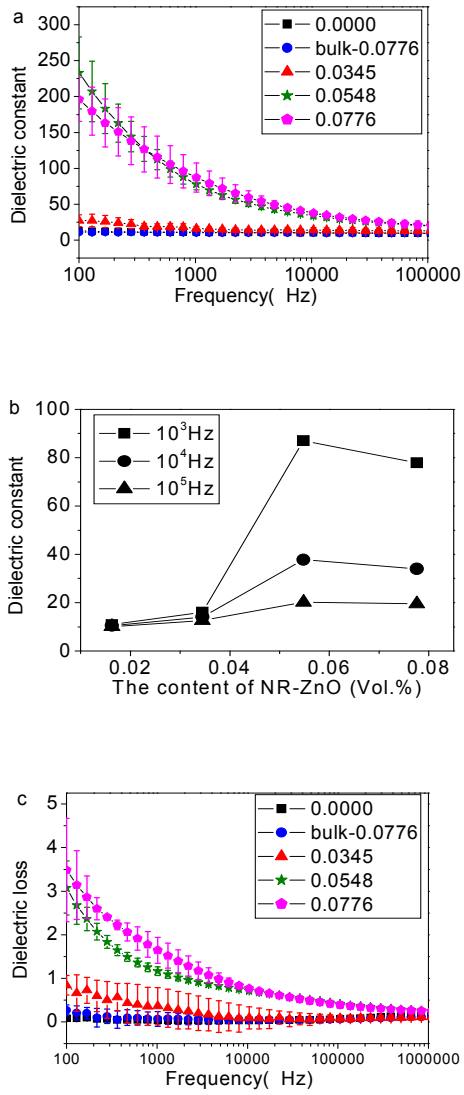

Figure 3. Dielectric constant (a) and dielectric loss (c) of the composites measured at different frequencies with different volume ratio at room temperature and (b) is the relationship of the dielectric constants with the filler contents.

Percolation theory can be employed to explain the enhancement in the dielectric constant. For the composites, the

variation of dielectric constant with the concentration of NR-ZnO can be divided into three stages. Initially, the dielectric constant rises gradually with the increasing NR-ZnO contents in the composites layers, because the microcapacitance structures between the two inorganic layers are not formed in low content of NR-ZnO. Subsequently, the percolation threshold is visible, at a critical volume concentration f_{NR-ZnO} =0.0548, where the dielectric constant abruptly increases. At this stage, the conduction behavior of the composites is also controlled by the concentration of the conducting NR-ZnO phase in the composites layer. Finally, the dielectric constant decreases due to a significant conductive network formation. The conductive network in the composites makes the composite become the conducting material and this leads to a high leakage current in the composite, so the dielectric constant decreases. While the dielectric constant of NR-ZnO/PVDF increases nonlinearly with the increasing volume ratio, when the volume ratio is 0.0548, the dielectric constant reaches its maximum. The percolation threshold of the two-phase random composite should be about f_c = 0.16 if the conducting fillers are sphere particles:[18]

$$\varepsilon = \varepsilon_0 \left| \frac{f_c - f_{NR-ZnO}}{f_c} \right|^{-q} \quad (1)$$

Where ε_0 is the dielectric constant of the PVDF matrix, f_{NR-ZnO} is the volume ratio of the NR-ZnO, f_c is the percolation threshold, and q is a critical exponent of about 1. The experimental values of the dielectric constant are in good agreement with Eq. (1), with f_c≈0.0717 and q≈0.8670. It is higher than the percolation threshold of R-ZnO/PVDF composite (f_c =0.0661)[41] and the carbon fiber/polymer (f_c =0.074). [42]

Temperature dependence of the dielectric constant and dielectric loss of composites in the neighbor (volume 0.0776) of percolation threshold is shown in **Figure 4**. Dielectric constant of the composites changing with temperature curves is consistent (shown in **Figure 4a**). At low frequency, for example, at 10^2 Hz, the dielectric constant quickly increased above 100 °C, because the molecules have enough time to be polarized; while, at high frequency, the composite exhibits good thermal stability at the frequency above 10^4 Hz, the polarization of molecules does not have enough time to catch up with the change of applied electrical field, thus the composite shows weak dependence of dielectric constant on temperature. For the dielectric loss of the composites changing with temperature curves (shown in **Figure 4b**) is also most the same with the dielectric constant; dielectric loss of the composite shows weak dependence of on temperature from 20°C to 100°C, and then increases from 110 °C to 140°C. For comparison, the temperature dependence of the dielectric constant and dielectric loss of pure PVDF is shown in **Figure S6**, both the dielectric constant and dielectric loss of PVDF increase with the increasing temperature from 20°C to 130°C.

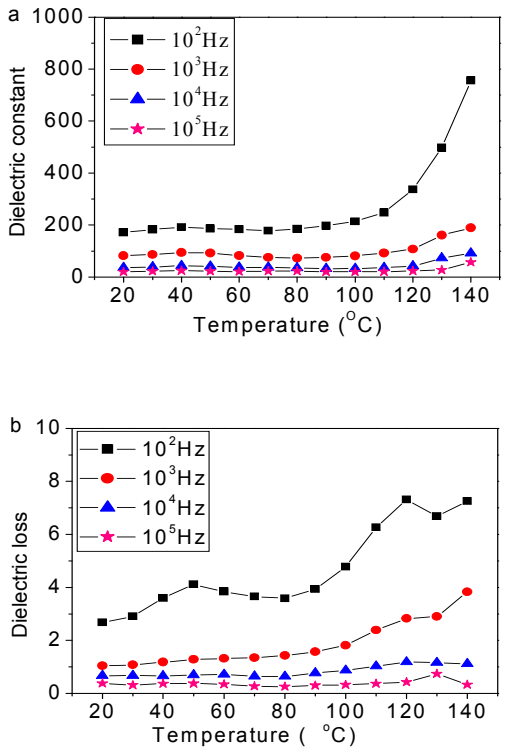

Figure 4. Dielectric constants (a) and Dielectric loss (b) of the NR-ZnO/PVDF composites with the volume concentration 0.0776 in the neighbor of percolation threshold: At 10^2 Hz, 10^3 Hz, 10^4 Hz and 10^5 Hz vs. temperature.

In order to investigate the microwave absorption properties of the products, specimens were prepared by uniformly mixing different quanitity NR-ZnO with wax or PVDF and pressing the mixture into a cylindrical shape with 7.00 mm outer diameter and 3.04 mm inner diameter for measurement. The complex permittivity and permeability of the composites were measured by using the transmission/reflection coaxial line method.[26] The frequency dependence relative permittivity for several materials

is investigated and shown in **Figure** 5. The real NR-ZnO/PVDF composites increase in general with the increasing loading content Figure 5a, which is higher than that of pure PVDF (about 3.0 at 2 GHz), while the permittivities of the composite with filler content 10 wt% is higher than that of 15 wt% in the frequency from 7.52 GHz to 14.80 GHz. It indicated that the introduction of NR-ZnO into PVDF can greatly enhance the dielectric constant of the PVDF composite at high frequency from 2 GHz to 18 GHz, which is the same with the CuS complex nanostructures;[36] the enhanced permittivities can be ascribed to the synergistic effect, which has been reported in previous report.[36, 43-45] And the imaginary permittivities of NR-ZnO/PVDF composites with 10 wt% (**Figure 5b**) are also higher than that of the composites with filler content 15 wt% in the higher frequency with two sharp peaks, we think that, one of the two peaks is intrinsic peak and the other is due to the synergistic reaction between NR-ZnO and PVDF, which is also confirmed by previous report.[36, 43-45]

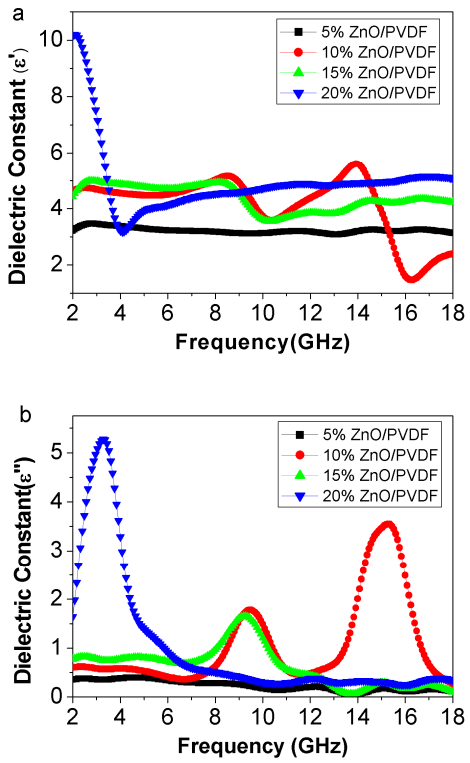

Figure 5. Measured frequency dependence of (a) real parts and (b) imaginary parts of permittivities.

We calculated the dielectric loss tangent of NR-ZnO/PVDF composites with different loadings (as shown in **Figure** S7). All the dielectric loss of the samples is higher than that of pure PVDF at the considered frequency. Therefore, the increasing loading of NR-ZnO results in an enhancement of the dielectric loss. But the nanocomposite with loading 10 wt% of synthesized NR-ZnO increases rapidly and shows two stronger dielectric loss peaks.

We also calculated the reflection loss (RL) coefficients of these materials based on the measured relative complex permittivity and permeability values. The RL coefficient (dB) of electromagnetic wave (normal incidence) at the surface of a single-layer material backed by a perfect conductor at a given frequency and layer thickness can be defined with the following equations according to transmission line theory:[46]

$$Z_{in} = \sqrt{\frac{\mu_r}{\varepsilon_r}} \tanh\left[j\left(\frac{2f\pi d}{c}\right)\sqrt{\mu_r \varepsilon_r}\right] \quad (2)$$

$$R = 20\log\left|\frac{Z_{in}-1}{Z_{in}+1}\right| \quad (3)$$

where Z_{in} is the input impedance of the absorber, Z_0 the impedance of free space, μ_r the relative complex permeability (ZnO is not a magnetic material, the μ_r values of NR-ZnO are regarded as 1), ε_r the complex permittivity, f the frequency of microwaves, d the thickness of the absorber, and c the velocity of light. Based on above equations, the reflection losses of different samples were all calculated and shown in **Figure 6,** show that the RLs of NR-ZnO/PVDF with different loading contents (from 5 wt % to 20 wt %) with the thinckness 3 mm, the NR-ZnO/wax with loading content of 10 wt% was also shown in this picture. For the NR-ZnO/wax composite with the loading content 10 wt%, there is no obvious RL peak can reach –5 dB in the frequency from 2 GHz to 18 GHz; while, for the NR-ZnO/PVDF with the same filler content, there are two sharp peaks: -15.90 dB at 6.60 GHz and -25.44 dB at 16.48 GHz, respectively; Comparing the RL values between these two samples, we find the enhancement in wave absorption of NR-ZnO/PVDF composite is obvious when the loading content is 10 wt%; Even taking RL values of pure PVDF samples into consideration, the wave absorption properties of NR-ZnO/PVDF are much better than NR-ZnO/wax. What's more, RL value of NR-ZnO/PVDF is higher than the numerical addition of NR-ZnO/wax with loading content 10 wt% and pure PVDF (Shown in **Figure S8**), indicating that the enhanced wave-absorption properties of NR-ZnO/PVDF are not just physical addition of NR-ZnO and PVDF. Furthermore, comparing with other composites with the different concentration, it is noted that only the NR-ZnO/PVDF with the loading content 10 wt% shows two minimum RL peaks: -15.90 dB at 6.60 GHz and -25.44 dB at 16.48 GHz; for the NR-ZnO/PVDF with the loading content 5 wt%, there is no RL peak at the frequency from 2 GHz to 18 GHz; for the NR-ZnO/PVDF with the loading content 15 wt%, there is only one absorption peak at 9.29 GHz, and the minimum RL can just reach -13.16 dB; while; for the NR-ZnO/PVDF composites with

the loading content 20 wt%, there is only a RL peak at the frequency 8.72 GHz, and the minimum RL just reaches -2.80 dB; these results also clearly demonstrate that the addition of NR-ZnO into PVDF can greatly enhance the wave absorption properties, especially when the loading is relatively as low as 10 wt%; In fact, the wave absorption ability of the composites with loading content 15 wt% and 20 wt% samples led to a worse reflection, and the relationship between wave absorption properties and the loading content in NR-ZnO/PVDF composite trends to be more complex: higher loading does not correspond to the stronger absorption peaks; the wave absorption intensity increases along with loadings when the loading is relative low; nevertheless, when the loading increased to a established value, the wave absorption intensity will reach maximum value and turn to decrease. The same phenomenon about CuS was also reported by us.[36, 45]

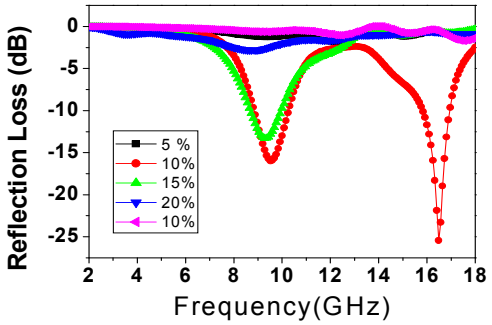

Figure 6. The reflection losses of different samples with the thickness of 3 mm.

The three-dimensional presentations of RL (**Figure 7a, b, c and d**) show the calculated theoretical RLs of the NR-ZnO/PVDF composites with different thickness (2-5 mm) in the range of 2-18 GHz with the loading of 5 wt%, 10 wt%, 15 wt% and 20 wt%, respectively. It indicates that the microwave absorbing properties and the minimum RLs corresponding to the maximum absorptions gradually appeared in different frequency can be tunable by controlling the thickness of the absorbers. While, the maximum absorptions increase with the increasing loading content from 0 to 10wt%, and then decrease. For the NR-ZnO/PVDF composites with the loading of 10 wt% shown in **Figure 7b**, when the absorbers with a thickness of 3.0 mm, there are two peaks, which can reach -15.90 dB at 6.60 GHz and -25.44 dB at 16.48 GHz, respectively, and the stronger peaks can also be adjusted by the thickness.

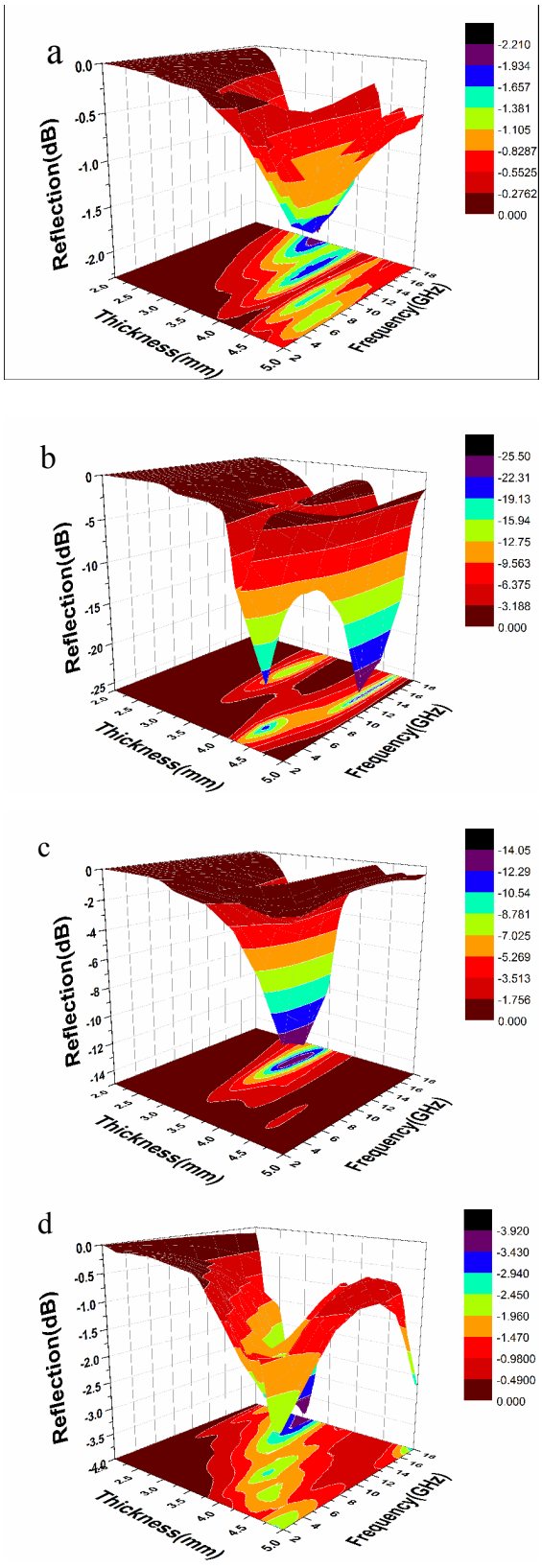

Figure 7. Three-dimensional presentations of RL of NR-ZnO/PVDF composites with loading 5 wt% (a); 10 wt% (b); 15 wt%(c) and 20 wt% (d).

For our composites, the enhaced mechanism is not clear; the reflection loss behaviors of materials usually depend on their loss mechanisms, which are determined by their nature, shape, size and microstructures.[26, 47] In the present work, there are several mechanisms such as Debye dipolar relaxation, which can account for the efficient microwave absorption properties of NR-ZnO/PVDF composite.That is, Debye dipolar relaxation is an crucial mechanism for inorganic-organic composite to absorb microwave as we introduced before.[39] As we know, the relaxation process is usually caused by the delay in molecular polarization with respect to a changing electric field in a dielectric medium. **Figure S9** shows the ε'-ε'' curve of the different samples. If Debye relaxation process accounts for the dielectric loss behavior, the relationship between ε' and ε'' can be deduced as:

$$(\varepsilon' - \frac{\varepsilon_s + \varepsilon_\infty}{2})^2 + (\varepsilon'')^2 = (\frac{\varepsilon_s - \varepsilon_\infty}{2})^2 \quad (4)$$

Thus, the plot of ε' versus ε'' would be a single semicircle, generally denoted as the Cole–Cole semicircle. For our composite, we conclude that the Debye relaxation process may take major responsibility for its dielectric loss behavior. As shown in **Figure S9**, for the Figure **S9a**, there is only Cole-Cole semicircles in the ε'-ε'' curves for the pure PVDF, which is the native relaxation of PVDF; for **Figure S9b**, there are many obvious Cole-Cole semicircles in the ε'-ε'' curves of PVDF with a loading of 5 wt %, indicating that at this stage, NR-ZnO are anomalously filled in PVDF and not connected, and formed a lot of local debye relaxation process; while,when the loading increased to 10 wt% , shown in **Figure S9c,** there are one big Cole-Cole semicircle and one small one in their ε'-ε'' curves, and at this stage, the Debye relaxation process of composite is due to the pure PVDF and the synergistic reaction between the NR-ZnO and PVDF, synergistic reaction acts as a overall effect action and the different NR-ZnO has interaction with others but not contects with others. When the content reaches 15 wt%; shown in **Figure S9d**, there is one big Cole-Cole semicircle and some small ones, the Debye relaxation process of composite is still due to the pure PVDF and the synergistic reaction between the NR-ZnO and PVDF, but some NR-ZnO contected with each other, and formed some local increment; which increased the number of Cole-Cole semicircle; while, when the content increased to 20 wt%; shown in **Figure S9e**, the composite is a conductor as a whole, and there are two Cole-Cole semicircles, of which one is due to the pure PVDF, and the other is the electric loss.

Conclusion

In summary, percolative composites ZnO/PVDF with enhanced dielectric properties and absorption properties based on PVDF and NR-ZnO, which is synthesized by controlling the addition of hydrazine hydrate with a simple wet chemical method, have been prepared by a simple hot press methd. The dielectric constant of the composite with f_{NR-ZnO} =0.0548 can reach 196 at 10^2 Hz, and the enhanced mechanism is explained by the percolative theory and the good thermal stability is still kept. It also confirmed that this method is effective to acquire high dielectric composite with high dielectric constant and excellent thermal stability composites with low inorganic filler content in industry. The reflection loss of the composite with the filler content 10 wt% appears two peaks that can reach -15.90 dB at 6.60 GHz and -25.44 dB at 16.48 GHz, respectively, which confirmed that this kind of composite is a promising wave-absorbing material. The increased mechanism of absorption properties was also explained by Debye relaxation theory.

Acknowledgment. This project was financially supported by the National Basic Research Program of China (2010CB934700) and the National Natural Science Foundation of China (Nos. 51102223, 50725208 and 51132002).

[a]*Key Laboratory of Bio-Inspired Smart Interfacial Science and Technology of Ministry of Education, School of Chemistry and Environment, Beihang University, Beijing 100191, PR China. wanggsh@buaa.edu.cn*
[b]*School of Materials Science and Engineering, Beijing Institute of Technology, Beijing 100081, China.*

† Electronic Supplementary Information (ESI) available: details of any supplementary information available should be included here]. See DOI: 10.1039/b000000x/

Reference

1. Z. L. Wang, *Journal of Physics: Condensed Matter*, 2004, **16**, R829.
2. Z. Fan, D. Wang, P.-C. Chang, W.-Y. Tseng and J. G. Lu, *Applied Physics Letters*, 2004, **85**, 5923.
3. P. Gao and Z. L. Wang, *The Journal of Physical Chemistry B*, 2002, **106**, 12653-12658.
4. Y. He, B. Yang and G. Cheng, *Catalysis today*, 2004, **98**, 595-600.
5. B. Liu and H. C. Zeng, *Journal of the American Chemical Society*, 2003, **125**, 4430-4431.
6. S. K. Sharma, A. Rammohan and A. Sharma, *Journal of colloid and interface science*, 2010, **344**, 1-9.
7. K. Ueda, H. Tabata and T. Kawai, *Applied Physics Letters*, 2001, **79**, 988.
8. J. J. Wu and S. C. Liu, *Advanced Materials*, 2002, **14**,

215-218.
9. B. Yao, Y. Chan and N. Wang, *Applied Physics Letters*, 2002, **81**, 757-759.
10. Z. Wang, T. Hu, L. Tang, N. Ma, C. Song, G. Han, W. Weng and P. Du, *Applied Physics Letters*, 2008, **93**, 222901.
11. J. Xu and C. Wong, *Applied Physics Letters*, 2005, **87**, 082907.
12. H. P. Xu and Z. M. Dang, *Chemical physics letters*, 2007, **438**, 196-202.
13. H. Stoyanov, D. Mc Carthy, M. Kollosche and G. Kofod, *Applied Physics Letters*, 2009, **94**, 232905.
14. K. Han, Q. Li, Z. Chen, M. R. Gadinski, L. Dong, C. Xiong and Q. Wang, *Journal of Materials Chemistry C*, 2013, **1**, 7034-7042.
15. S. Tjong and G. Liang, *Materials chemistry and physics*, 2006, **100**, 1-5.
16. Z. Dang, L. Fan, S. Zhao and C. Nan, *Materials research bulletin*, 2003, **38**, 499-507.
17. M. Kawasumi, N. Hasegawa, M. Kato, A. Usuki and A. Okada, *Macromolecules*, 1997, **30**, 6333-6338.
18. S. H. Yao, J. K. Yuan, Z. M. Dang and J. Bai, *Materials Letters*, 2010, **64**, 2682-2684.
19. M. Molberg, D. Crespy, P. Rupper, F. Nüesch, J. A. E. Månson, C. Löwe and D. M. Opris, *Advanced Functional Materials*, 2010, **20**, 3280-3291.
20. T. I. Yang, R. N. Brown, L. C. Kempel and P. Kofinas, *Journal of Nanoparticle Research*, 2010, **12**, 2967-2978.
21. Z. M. Dang, S. H. Yao, J. K. Yuan and J. Bai, *The Journal of Physical Chemistry C*, 2010, **114**, 13204-13209.
22. J. Hong, P. Winberg, L. Schadler and R. Siegel, *Materials Letters*, 2005, **59**, 473-476.
23. L. Brus, *Applied Physics A*, 1991, **53**, 465-474.
24. J. Wang, M. S. Gudiksen, X. Duan, Y. Cui and C. M. Lieber, *Science*, 2001, **293**, 1455-1457.
25. G. Wang, Y. Deng, Y. Xiang and L. Guo, *Advanced Functional Materials*, 2008, **18**, 2584-2592.
26. G. Wang, Z. Gao, S. Tang, C. Chen, F. Duan, S. Zhao, S. Lin, Y. Feng, L. Zhou and Y. Qin, *ACS nano*, 2012, **6**, 11009-11017.
27. S. Meng, X. Guo, G. Jin, Y. Wang and S. Xie, *Journal of Materials Science*, 2012, **47**, 2899-2902.
28. R. Che, L. M. Peng, X. F. Duan, Q. Chen and X. Liang, *Advanced Materials*, 2004, **16**, 401-405.
29. M. Kim, K. Sohn, H. B. Na and T. Hyeon, *Nano Letters*, 2002, **2**, 1383-1387.
30. L. Wang, H. Wei, Y. Fan, X. Gu and J. Zhan, *The Journal of Physical Chemistry C*, 2009, **113**, 14119-14125.
31. G. S. Wang, L. Z. Nie and S. H. Yu, *RSC Advances*, 2012, **2**, 6216-6221.
32. S. He, G. S. Wang, C. Lu, X. Luo, B. Wen, L. Guo and M. S. Cao, *ChemPlusChem*, 2013, **78**, 250-258.
33. H. B. Lin, M. S. Cao, Q. L. Zhao, X. L. Shi, D. W. Wang and F. C. Wang, *Scripta Materialia*, 2008, **59**, 780-783.
34. M. S. Cao, X. L. Shi, X. Y. Fang, H. B. Jin, Z. L. Hou, W. Zhou and Y. J. Chen, *Applied Physics Letters*, 2007, **91**, 203110.
35. Y. Chen, M. Cao, T. Wang and Q. Wan, *Applied Physics Letters*, 2004, **84**, 3367-3369.
36. S. He, G. S. Wang, C. Lu, J. Liu, B. Wen, H. Liu, L. Guo and M.-S. Cao, *Journal of Materials Chemistry A*, 2013, **1**, 4685-4692.
37. Y. Deng, Y. Zhang, Y. Xiang, G. Wang and H. Xu, *Journal of Materials Chemistry*, 2009, **19**, 2058-2061.
38. Z. M. Dang, J. K. Yuan, S. H. Yao and R. J. Liao, *Advanced Materials*, 2013, **25**, 6334-6365.
39. Z. de Chen, G. S. Wang, S. He, L. Guo and M.-S. Cao, *Journal of Materials Chemistry A*, 2013,15996.
40. G. S. Wang, Y. Deng and L. Guo, *Chemistry-A European Journal*, 2010, **16**, 10220-10225.
41. G. S. Wang, *ACS Applied Materials & Interfaces*, 2010, **2**, 1290-1293.
42. Z. M. Dang, J. P. Wu, H. P. Xu, S. H. Yao, M. J. Jiang and J. Bai, *Applied Physics Letters*, 2007, **91**, 072912.
43. G. S. Wang, X. J. Zhang, Y. Z. Wei, S. He, L. Guo and M. S. Cao, *Journal of Materials Chemistry A*, 2013, 7031-7036.
44. G. S. Wang, S. He, X. Luo, B. Wen, M. M. Lu, L. Guo and M. S. Cao, *RSC Advance.*, 2013, **3**, 18009-18015.
45. X. J. Zhang, G. S. Wang, Y. Z. Wei, L. Guo and M. S. Cao, *Journal of Materials Chemistry A*, 2013, **1**, 12115-12122.
46. M. S. Cao, X. L. Shi, X. Y. Fang, H. B. Jin, Z. L. Hou, W. Zhou and Y. J. Chen, *Applied Physics Letters*, 2007, **91**,203110.
47. X. F. Zhang, X. L. Dong, H. Huang, Y. Y. Liu, W. N. Wang, X. G. Zhu, B. Lv, J. P. Lei and C. G. Lee,

Applied Physics Letters, 2006, **89**,053115.